Transformation kinetics of chlorinated ethenes by Methylosinus trichosporium OB3b and detection of unstable epoxides by on-line gas chromatography

van Hylckama Vlieg, Johan. E.T.; Koning, Wim de; Janssen, Dick B.

Published in:
Applied and environmental microbiology

Publication date:
1996

APPLIED AND ENVIRONMENTAL MICROBIOLOGY, Sept. 1996, p. 3304–3312 Vol. 62, No. 9
0099-2240/96/$04.00+0

Transformation Kinetics of Chlorinated Ethenes by *Methylosinus trichosporium* OB3b and Detection of Unstable Epoxides by On-Line Gas Chromatography

JOHAN E. T. VAN HYLCKAMA VLIEG, WIM DE KONING, AND DICK B. JANSSEN*

Department of Biochemistry, Groningen Biomolecular Sciences and Biotechnology Institute, University of Groningen, 9747 AG Groningen, The Netherlands

Received 29 February 1996/Accepted 26 June 1996

A rapid and accurate method for the determination of transformation kinetics of volatile organic substrates was developed. Concentrations were monitored by on-line gas chromatographic analysis of the headspace of well-mixed incubation mixtures. With this method, the kinetics of transformation of a number of C_1 and C_2 halogenated alkanes and alkenes by *Methylosinus trichosporium* OB3b expressing particulate methane monooxygenase or soluble methane monooxygenase (sMMO) were studied. Apparent specific first-order rate constants for cells expressing sMMO decreased in the order of dichloromethane, vinyl chloride, *cis*-1,2-dichloroethene, *trans*-1,2-dichloroethene, 1,1-dichloroethene, trichloroethene, chloroform, and 1,2-dichloroethane. During the degradation of trichloroethene, *cis*-1,2-dichloroethene, *trans*-1,2-dichloroethene, and vinyl chloride, the formation of the corresponding epoxides was observed. The epoxide of vinyl chloride and the epoxide of trichloroethene, which temporarily accumulated in the medium, were chemically degraded according to first-order kinetics, with half-lives of 78 and 21 s, respectively. Cells expressing sMMO actively degraded the epoxide of *cis*-1,2-dichloroethene but not the epoxide of *trans*-1,2-dichloroethene. Methane and acetylene inhibited degradation of the epoxide of *cis*-1,2-dichloroethene, indicating that sMMO was involved.

Trichloroethene (TCE), vinyl chloride (VC), 1,2-dichloroethane, and other chlorinated ethenes and ethanes are important environmental pollutants. TCE has been widely used as a degreasing agent. VC and 1,1-dichloroethene (1,1-DCE) are used for the synthesis of synthetic resins. Under aerobic conditions, VC (16) and several chlorinated alkanes (19, 22) have been shown to serve as sole sources of carbon and energy for a bacterial culture. For TCE and DCEs, cometabolic degradation by organisms expressing monooxygenases or dioxygenases during growth on methane (18, 28, 35, 37), propane (40), propene (9), isoprene (10), ammonia (2), or toluene (26, 41) has been reported. There is a strong interest in using such organisms for the bioremediation of soil, groundwater, or air contaminated with chlorinated aliphatics. TCE, VC, and *cis*-1,2-DCE are of special importance in this respect since they can also be produced anaerobically in contaminated sites from perchloroethene.

Several factors determine the suitability of organisms for application in a cometabolic remediation process. A broad substrate range is desirable, since polluted groundwater or other waste streams often contain more than one contaminating compound. The kinetics of degradation are also important since high degradation rates may allow high volumetric degradation capacities, and high substrate affinities make it easier to obtain low effluent concentrations. However, the kinetics of cometabolic conversion are often complex and can be influenced by a number of factors. Cometabolic degradation can be regarded as an unavoidable side reaction, and this can be a disadvantage for the organism. Energy may be lost without any benefit to the cell, as, for instance, in the use of NADH in oxygenase reactions which yield products that are not further metabolized. Competitive inhibition between the growth substrate and the pollutant, resulting in a reduction of degradation rates, can occur (1, 23). Furthermore, cometabolic transformation of chlorinated hydrocarbons can result in the generation of reactive compounds that inactivate the cell and thus limit the transformation capacity (1, 27). For important industrial pollutants such as chloroform and TCE, however, cometabolic transformation is the only available possibility for an aerobic bioremediation process.

Methanotrophs are good candidates for such applications, since they are capable of degrading a broad range of halogenated aliphatics (1, 12, 27, 28, 35, 37). The methane monooxygenases (MMO) that are expressed by these organisms can be divided into two classes. All methanotrophs tested are able to form a particulate enzyme (pMMO). Under copper limitation, only some strains such as *Methylosinus trichosporium* OB3b, *Methylococcus capsulatus* (Bath) (34), and *Methylomonas methanica* 68-1 (35) are able to form a soluble enzyme (sMMO), which has a broader substrate range and is capable of oxidizing TCE and other chlorinated aliphatics. Several bench-scale reactors have been constructed, such as biofilm reactors (3, 11) and plug flow reactors (36), in which the removal of TCE by these organisms has been studied.

The oxidation of chlorinated ethenes by sMMO results in generation of the corresponding epoxides. These reactions are similar to the oxidation of chlorinated ethenes by cytochrome P-450 in eukaryotes. The epoxides are electrophilic compounds, and from studies of eukaryotic systems, it is known that a variety of secondary reactions, such as alkylation of biomolecules or hydrolysis to *vic*-diols or acylhalides, may occur. The reactivity of the epoxides and their degradation products are considered to be responsible for the toxicity of chlorinated ethenes. The metabolism of VC in mammals has been studied extensively because of its mutagenic and carcinogenic potential (24, 31). From the DNA alkylation products that have been isolated from animals exposed to VC, it could be

* Corresponding author. Mailing address: Department of Biochemistry, Groningen Biomolecular Sciences and Biotechnology Institute, University of Groningen, Nijenborgh 4, 9747 AG Groningen, The Netherlands. Phone: 31 50 3634108. Fax: 31 50 3634165.

derived that the epoxide generated after the oxidation of VC, chloroepoxyethane (VC epoxide), is the ultimate carcinogenic product of VC. TCE is a suspected carcinogen, but little information is available about covalent modifications of DNA due to the metabolism of this compound.

Toxicity related to conversion of chlorinated ethenes has also been observed in bacteria (12, 27). However, little is known about the kinetics of degradation of the epoxides, since their instability in aqueous solutions makes it difficult to perform accurate quantitative analysis.

In this article, we describe the on-line monitoring of volatile substrates and oxidation products by gas chromatography (GC). The method was used to determine the kinetics of degradation of various halogenated aliphatics by *Methylosinus trichosporium* OB3b expressing pMMO or sMMO and made possible the detection of the corresponding epoxides. The results showed that significant amounts of all epoxides, except 1,1-dichloroepoxyethane (1,1-DCE epoxide), leave the cell. Furthermore, it was found that *cis*-1,2-dichloroepoxyethane (*cis*-1,2-DCE epoxide) is actively transformed by sMMO, whereas other structurally related epoxides are not substrates for sMMO.

MATERIALS AND METHODS

Nomenclature. The following parameters are used in this paper: a, constant relating peak area to substrate concentration; C, the substrate concentration (micromolar); f, the fraction of oxidized chlorinated ethene that is converted to epoxide (dimensionless); H, Henry's gas-liquid partition coefficient (milliliters of gas milliliter of liquid^{-1}); k_1, the specific first-order degradation rate constant (milliliters minute^{-1} milligram of cells^{-1}); k, the chemical first-order degradation rate constant (minute^{-1}); k_La, mass-transfer rate coefficient (minute^{-1}); K_m, the Michaelis-Menten constant (micromolar); K_s, the Monod constant (micromolar); r_{max}, the maximal specific substrate conversion rate (micromoles minute^{-1} milligram of cells^{-1}); r, specific substrate conversion rate (micromoles minute^{-1} milligram of cells^{-1}); S, amount of substrate (micromoles); μ_{max}, the maximal specific growth rate (minute^{-1}); V, volume (milliliter); X, the concentration of cells (milligram of cells [dry weight] milliliter^{-1}); Y, growth yield (milligram of cells [dry weight] micromole^{-1}). Subscripts denote the following parameters; g, gas phase; l, liquid phase; O, epoxide; S, substrate; X, biomass; 0, at time zero.

Organism and growth conditions. *Methylosinus trichosporium* OB3b was obtained from the National Collection of Industrial and Marine Bacteria, Aberdeen, United Kingdom. The organism was grown continuously in a 3-liter fermentor with methane as the sole carbon source at a dilution rate of 0.03 h^{-1}. Mineral medium (MMF) was essentially the same as the medium described by Janssen et al. (18). Only Na_2HPO_4 was replaced by KH_2PO_4, and the medium in the supply vessel was acidified to pH 3.0 with H_2SO_4 to prevent formation of precipitates. Copper was omitted from the medium to allow expression of sMMO.

The pH was 6.9 and continuously regulated by titration with 1 N NaOH. Other conditions were as follows: working volume, 2,350 ml; temperature, 30°C; impeller speed, 1,250 rpm; methane flow rate, 6 to 8 ml min^{-1}; air flow rate, 55 to 60 ml min^{-1}. The dissolved oxygen tension was 25 to 50% air saturation. The sterile air-methane mixture was bubbled through the fermentor. The biomass concentration was 0.3 to 0.4 mg of cells ml^{-1}.

On-line monitoring of substrate concentrations and transformation experiments. Degradation rates of chlorinated aliphatics were determined by on-line analysis of their concentrations in the headspace of incubation mixtures. The experimental setup consisted of a 120-ml jacketed glass incubation vessel that was temperature controlled at 30°C. Gas was continuously withdrawn from the headspace with a micromembrane pump (model NMP 02LU; KNF Neuberger GmbH, Freiburg-Munzingen, Germany). After passage through a Valco 6 port sampling injector (Vici AG, Schenkon, Switzerland) to which a 35-μl sample loop was connected, the gas was injected back into the magnetically stirred liquid phase in the incubation vessel through an open-ended tube with an internal diameter of 0.08 mm and a flow rate of approximately 200 ml min^{-1}. This allowed rapid mass transfer between the gas and liquid phases. Stainless-steel tubing and a glass-embedded magnetic stirrer were used, since sorption was observed with synthetic materials. With time intervals of 0.25 to 1 min, the contents of the sample loop were injected into the GC and analyzed isothermally at 60 to 130°C. The GC (type CP 9001; Chrompack, Middelburg, The Netherlands) was equipped with a CPsil 5 CB column (Chrompack; length, 25 m; inner diameter, 0.53 mm; film thickness, 5 μm) and a flame-ionization detector. Helium was used as the carrier gas (26 ml min^{-1}), and the flame ionization detector was supplied with hydrogen (30 ml min^{-1}), air (270 ml min^{-1}), and N_2 (30 ml min^{-1}). The high sensitivity of the GC analysis allowed the determination of concentrations as low as 0.05 μM in the headspace. Calibrations were carried out by adding a well-defined amount of substrate to the incubation system. In this way, errors in the estimations of the total mass and transformation rates were minimized.

To evaluate the mass-transfer characteristics, the k_La was determined by adding a pulse of TCE to the liquid phase or to the headspace of a reaction vessel which contained 25 ml of MMF medium. The concentration in the headspace was monitored until equilibrium was reached. The substrate concentration and its dependence on the k_La in time are described by:

$$\frac{dC_g}{dt} = -k_La\frac{V_i}{V_g}\left(\frac{C_g}{H} - \frac{S_{tot}}{V_l} + \frac{C_gV_g}{V_l}\right) \quad (1)$$

which can be solved to give:

$$C_{g,t} = \frac{HS_{tot}}{V_l + HV_g} + \left(C_{g,0} - \frac{HS_{tot}}{V_l + HV_g}\right)e^{-K_La\left(\frac{V_l}{HV_g}+1\right)t} \quad (2)$$

where $C_{g,0}$ is 0 or S_{tot}/V_g when TCE was added to the liquid phase or gas phase, respectively.

The published Henry constants that were used for the calculations are as follows: methane, 33 (29); dichloromethane, 0.11; chloroform, 0.19; VC, 1.26; *cis*-1,2-DCE, 0.19; *trans*-1,2-DCE, 0.47; 1,1-DCE, 1.27; TCE, 0.51 (13). Other Henry constants were determined by analyzing a series of closed bottles of equal volume containing various amounts of MMF medium to which a fixed amount of epoxide was added. The Henry constants were calculated from a plot of the reciprocal peak area versus the liquid volume, which gives a straight line from which H can be calculated with:

$$\frac{1}{\text{area}} = -\frac{H-1}{HP}aV_l + a\frac{V_{tot}}{S_{tot}} \quad (3)$$

In this equation, a is a constant relating peak area to concentrations. The resulting values for the Henry coefficient were 0.011, 0.049, and 0.011 for *cis*-1,2-DCE epoxide, *trans*-1,2-dichloroepoxyethane (*trans*-1,2-DCE epoxide), and epoxyethane, respectively.

In a typical transformation experiment, 25 ml of cell suspension freshly taken from the fermentor was used. Formate and phosphate buffer (pH 6.9) were added to a final concentration of 20 mM. The cell suspension was incubated for 5 min at 30°C to allow the cells to generate enough reducing power to obtain the maximal initial degradation rate. Assays were started by adding 0.1 to 3 μmol of substrate either from a stock solution in water or as a gas. Cells were protected from light, since it was observed that cells rapidly inactivate when illuminated (38a). When cell densities did not exceed 0.5 mg of cells ml^{-1}, the activity of the cells remained constant for at least 2 h.

Chloride levels were determined by the colorimetric method of Bergmann and Sanik (5).

Calculation of transformation rates. At low substrate concentrations, where $S \ll K_m$, transformation follows first-order kinetics. In the case of equilibrium, volatile substrates will be distributed over the headspace and liquid phase according to the dimensionless Henry partition coefficient. In this case, the microbial degradation of the substrate can be described with:

$$\frac{dC_g}{dt} = -k_1XC_g\left(\frac{V_l}{V_l + HV_g}\right) \quad (4)$$

After integrating over time, this can be rewritten to:

$$C_{g,t} = C_{g,0}e^{-k_1X\frac{V_l}{V_l + HV_g}t} \quad (5)$$

These equations are only valid when mass-transfer limitation does not occur. When mass transfer plays a role, the headspace and liquid phase concentration can be described by:

$$\frac{dC_g}{dt} = -k_La\frac{V_l}{V_g}\left(\frac{C_g}{H} - C_l\right) \quad (6)$$

$$\frac{dC_l}{dt} = k_La\left(\frac{C_g}{H} - C_1\right) - k_1XC_l \quad (7)$$

The k_1 can be obtained by fitting a data set of headspace concentrations to equations 6 and 7. In case transformation proceeds according to Michaelis-Menten kinetics, equation 8 was used instead of equation 7:

$$\frac{dC_l}{dt} = k_La\left(\frac{C_g}{H} - C_l\right) - r_{max}X\left(\frac{C_l}{C_l + K_m}\right) \quad (8)$$

The concentration of epoxide over time is a function of the biological oxidation rate of the chlorinated ethene that is described by equations 6 and 7, with an extra factor f, which is the fraction of oxidized ethene that is converted to epoxide, and a term for the (chemical) first-order degradation rate of the ep-

oxide. Since chemical degradation of the epoxide will take place in the liquid phase according to first-order kinetics, the headspace concentration can be described by an equation analogous to equation 6, and the liquid-phase concentration of epoxide can be described by:

$$\frac{dO_l}{dt} = k_L a \left(\frac{O_g}{H} + O_l\right) + fk_1 XC_l - kO_l \quad (9)$$

in which O_g was determined by fitting the equation to the measured peak areas with a variable that related peak areas to concentrations.

In the case of competitive inhibition, the rate of substrate conversion is described by:

$$r = r_{\max}\left(\frac{C_l}{K_m\left(1 + \frac{l}{K_i}\right) + C_l}\right) \quad (10)$$

If the transformation of a chlorinated substrate follows first-order kinetics and transformation is competitively inhibited by methane, the relation between the observed k_1 and the methane concentration simplifies to:

$$k_{1,l} = k_{1,0}\left(\frac{K_i}{l + K_i}\right) \quad (11)$$

The K_i of methane on the conversion of *cis*-1,2-DCE epoxide was obtained by determining the k_1 value of *cis*-1,2-DCE epoxide degradation in the presence of various concentrations of methane. The methane concentrations in the liquid phase were calculated with equations 6 and 8. Since the methane concentration changed less than 5% as a result of bacterial consumption, it was assumed to be constant.

Data were fitted to analytical equations by nonlinear regression analysis in Sigma Plot (Jandel Scientific Software, San Rafael, Calif.) or by numerical integration by use of the episode routine in Scientist for Windows 2.0 (Micromath Scientific Software, Salt Lake City, Utah).

Preparation of *cis*- and *trans*-1,2-DCE epoxide. The compounds *cis*- and *trans*-1,2-DCE epoxide are not commercially available, and their half-lives in aqueous solutions are 72 and 30 h, respectively. Chemical synthesis is time-consuming and gives rather poor yields (14). We synthesized these epoxides with *Methylosinus trichosporium* OB3b. For this, cells were harvested from a continuous culture, centrifuged at 10,000 × *g* for 5 min, and resuspended in 25 ml of MMF medium containing 40 mM phosphate to a cell density of 20 mg of cells ml^{-1}. The suspension was transferred to the incubation vessel, and 5 to 10 pulses of 5 μl of *cis*- or *trans*-1,2-DCE were added. Degradation of the substrate and generation of the epoxide were monitored continuously. Repeated addition of formate and O_2 enabled optimal transformation. Transformation was stopped by the addition of $HgCl_2$ (0.1 mg ml^{-1}). The epoxides were removed from the suspension by bubbling N_2 gas at a flow rate of 20 ml min^{-1} through the suspension and subsequently trapped in a glass U-tube kept in liquid nitrogen.

The identity and purity of the isolated compound were checked with ^1H nuclear magnetic resonance. Therefore, 10 μl of the isolated compound was dissolved in 1 ml of $CDCl_3$, and 20 μl of TCE was added as an internal standard. The ^1H nuclear magnetic resonance spectrum showed two singlets at 5.07 and 6.46 ppm, corresponding to *trans*-1,2-DCE epoxide and TCE, respectively. The purity was estimated to be approximately 95%. The mixture was used to calibrate the GC by determining the *trans*-1,2-DCE epoxide/TCE molar response ratio of the flame ionization detector. This was calculated to be 0.43, meaning that the response of the detector to 1 equivalent of *trans*-1,2-DCE epoxide is 0.43 times the response caused by 1 equivalent of TCE. The response ratios of *trans*-1,2-DCE epoxide and *cis*-1,2-DCE epoxide were assumed to be equal. In all experiments, calibration with TCE was used to calculate the concentration of *trans*-1,2-DCE epoxide or *cis*-1,2-DCE epoxide.

Identification of chlorinated ethene epoxides. The products of the oxidation of chlorinated ethenes were identified by mass spectrometry with a type 5971 mass selective detector connected to a model HP 5890 GC (Hewlett-Packard) that was equipped with an HP5 column (length, 30 m; inner diameter, 0.25 mm; film thickness, 0.25 μm). Helium was used as a carrier gas (0.9 ml min^{-1}). Samples were taken from the headspace of degradation experiments as described for on-line GC analysis. The identity of *cis*-1,2-DCE and *trans*-1,2-DCE epoxide was confirmed by comparison of the retention times by GC with chemically synthesized standards (18). The unstable intermediates that accumulated in the headspace during degradation of VC and TCE were identified by the colorimetric method of Barbin et al. (4). For this, a reaction tube containing 2 ml of 100 mM 4-(4-nitrobenzyl)pyridine (PNBP) in ethylene glycol was introduced in the recirculating gas flow during a degradation experiment, to trap the unstable intermediates. Transformation experiments were carried out with 25 ml of cell suspension (0.5 mg of cells ml^{-1}). Reactions were started by the addition of 4.0 μmol of VC or 2.6 μmol of TCE. After complete degradation of the substrate, 1 ml of a mixture of Tris-acetate buffer (pH 7.4), 1 ml of acetone, and 3.2 ml of acetone-triethylamine (1:1, vol/vol) were added to the trapping mixture. The identity of the PNBP adducts was determined by analysis of their absorption spectra (200 to 700 nm) (data not shown).

The colorimetric assay was also used to estimate the concentration of epoxide in the liquid phase during the degradation of VC and TCE. A series of serum flasks containing a cell suspension was shaken vigorously. The cell density, the initial substrate concentrations, and the ratio of gas volume to liquid volume were identical to those used in the on-line experiments. The suspensions were quenched at different time points with 1 volume of benzene, and the concentrations of the epoxides were determined as described by Fox et al. (12). The extinction coefficients of PNBP adducts used for quantitation are 24 mM^{-1} cm^{-1} at 565 nm and 24 mM^{-1} cm^{-1} at 540 nm for VC epoxide and 1,1,2-trichloroepoxyethane (TCE epoxide), respectively (12, 15).

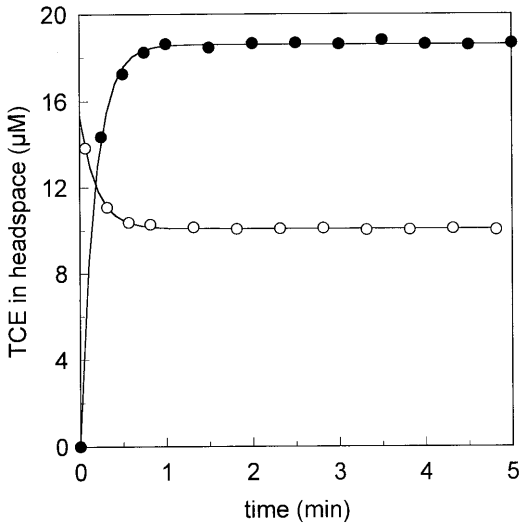

FIG. 1. Determination of $k_L a$ values for TCE in the on-line analysis system. TCE was injected in the liquid phase (2.65 μmol) (●) or in the headspace (1.46 μmol) (○). The data were fitted with equation 2. Input parameters: $H = 0.51$; $V_l = 25$ ml; $V_g = 95.3$ ml.

Chemicals. All gases were obtained from AGA Gas B.V. (Amsterdam, The Netherlands). Organic chemicals used in this study were obtained from Acros Chimica (Gael, Belgium), from Sigma Chemical Co. (St. Louis, Mo.), or Aldrich (Milwaukee, Wis.).

RESULTS

On-line headspace analysis. On-line headspace analysis is an attractive method for the determination of cometabolic transformation kinetics of volatile compounds. However, it is essential to evaluate to what extent the course of headspace and liquid-phase concentrations are influenced by mass-transfer limitation. The rate of gas-liquid mass transfer is determined by the mass-transfer rate coefficient ($k_L a$) and the Henry coefficient. The $k_L a$ of the incubation vessel was measured for TCE by adding a pulse of TCE to the liquid phase or the headspace (Fig. 1). The data were fitted with equation 2, and the $k_L a$ values for TCE were calculated to be 3.8 and 3.4 min^{-1} from fits of pulses added to the liquid phase and headspace, respectively.

The $k_L a$ of a compound is dependent on its diffusity and can be calculated for other compounds by multiplying the $k_L a$ obtained for TCE with the third root of the molecular weight of TCE relative to the molecular weight of the compound of interest (29). The $k_L a$ values that could thus be calculated for the other compounds used in this study are as follows: methane, 7.3 min^{-1}; epoxyethane, 5.2 min^{-1}; epoxypropane, 4.7 min^{-1}; 1,2-epoxybutane, 4.4 min^{-1}; *cis*-2,3-epoxybutane, 4.4 min^{-1}; *trans*-2,3-epoxybutane, 4.4 min^{-1}; VC, 4.6 min^{-1}; dichloromethane, 4.2 min^{-1}; 1,1-DCE, 4.4 min^{-1}; *cis*-1,2-DCE, 4.0 min^{-1}; *trans*-1,2-DCE, 4.0 min^{-1}; 1,2-dichloroethane, 4.0 min^{-1}; VC epoxide, 4.3 min^{-1}; *cis*-1,2-DCE epoxide, 3.8 min^{-1}; *trans*-1,2-DCE epoxide, 3.8 min^{-1}; TCE epoxide, 3.5 min^{-1}.

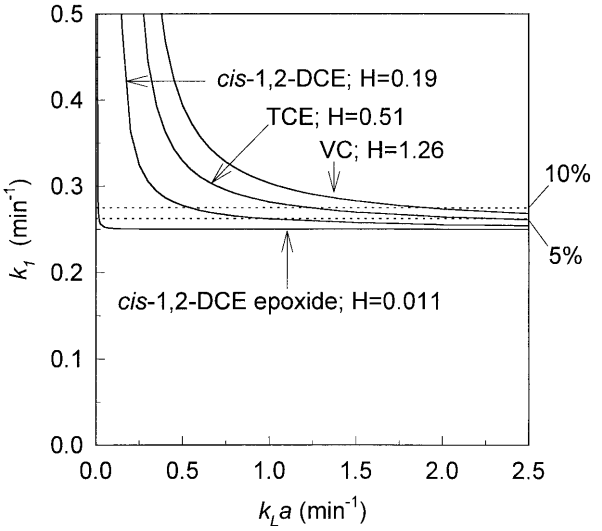

FIG. 2. Influence of mass-transfer limitation on the estimation of specific first-order transformation rate constants of compounds with different Henry coefficients. Substrate depletion curves were simulated with equation 5, where k_1 was set at 0.25 min^{-1} and X was set at 1.0 mg ml^{-1}. The simulated substrate depletion curves were then fitted with equations 6 and 7 assuming different k_La values. The k_1 values that were thus obtained are plotted as a function of the k_La. The dotted lines indicate the 5 and 10% error values (k_1 = 0.263 and 0.275 ml mg^{-1} min^{-1}, respectively).

The course of headspace and liquid-phase concentrations also depends on the Henry coefficient. A higher Henry coefficient will result in a larger influence of mass transfer on the course of the headspace concentration (i.e., a larger deviation from equilibrium). This influence was studied for various compounds with high or low Henry coefficients. For this, substrate depletion curves with a k_1 value of 0.25 min^{-1} and a biomass concentration of 1.0 mg ml^{-1}, assuming equilibrium, were simulated with equation 5. The resulting simulated datum points were fitted with equations 6 and 7 with various fixed k_La values. In Fig. 2, the k_1 values resulting from these fits are plotted as a function of the k_La. For the compound used in this study with the lowest Henry coefficient, *cis*-1,2-DCE epoxide (H = 0.011), the error in the k_1 value that is derived from the fit is less than 10% different from the k_1 that is derived assuming equilibrium, even if the k_La value was as low as 0.1 min^{-1} (0.4 times the value of k_1). For a compound with a very high Henry coefficient, such as VC (H = 1.26), the k_La value resulting in an error that is smaller than 10% is 2.0 min^{-1} (8 times the value k_1). This illustrates that equilibrium may be assumed if the k_La is about 10-fold larger than the value of k_1X.

Experimental data were routinely fitted by numerical integration by use of the equations in which mass transfer was implemented. Whenever possible, transformation experiments were carried out with cell densities resulting in first-order transformation rates at which mass-transfer limitation did not significantly influence the course of the headspace concentrations. Thus, problems due to inaccurate estimation of the k_La were minimized.

Transformation of halogenated compounds by *Methylosinus trichosporium* OB3b. The transformation kinetics of several C_1 and C_2 chlorinated aliphatics with cells expressing pMMO and cells expressing sMMO were determined by on-line GC analysis. Except for dichloromethane conversion with cells expressing sMMO, transformation of all compounds followed first-order kinetics at concentrations up to 30 μM.

As an example, substrate depletion curves obtained with cells expressing pMMO or sMMO are shown in Fig. 3. The conversion of dichloromethane with cells expressing pMMO followed first-order kinetics (Fig. 3A) and was fitted to equations 6 and 7. From this fit, a specific first-order transformation rate constant (k_1) of 0.67 ml min^{-1} mg of cells^{-1} was calculated. Transformation of dichloromethane with cells expressing sMMO did not follow first-order kinetics (Fig. 3B). By fitting headspace data to equations 6 and 8, describing Michae-

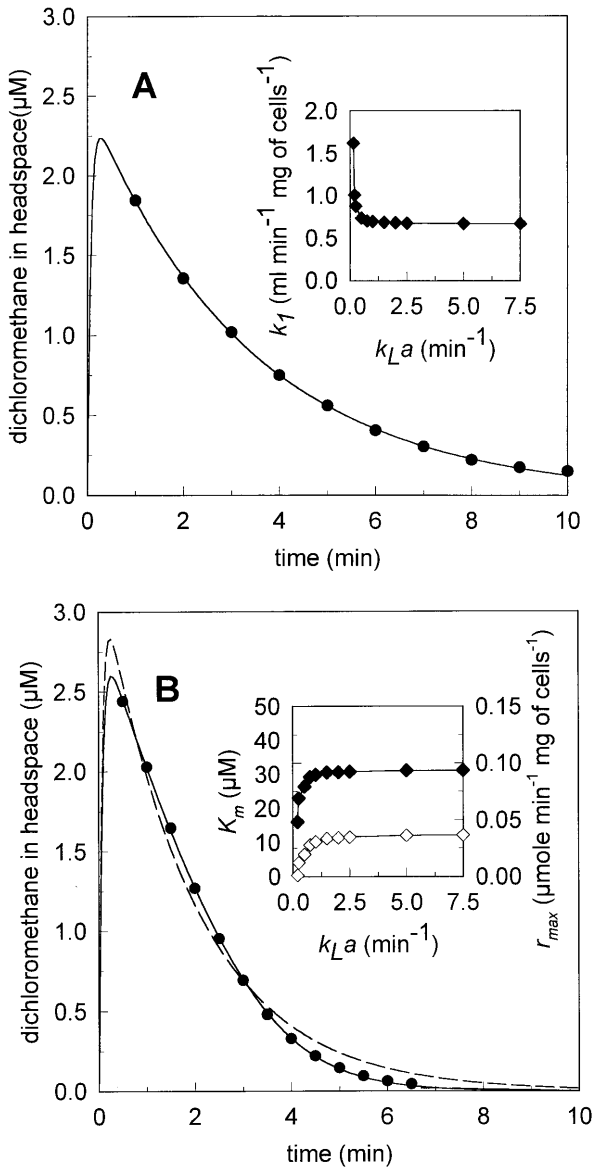

FIG. 3. Transformation of dichloromethane by cell suspensions of *Methylosinus trichosporium* OB3b and effect on parameter estimation. (A) Dichloromethane (●) depletion curve obtained with cells expressing pMMO. Transformation followed first-order kinetics, and the data were fitted with equations 6 and 7. Input parameters: H = 0.11; k_La, 4.2 min^{-1}; V_g = 94.8 ml; V_l = 25.5 ml; X = 0.63 mg of cells ml^{-1}. An optimal fit was obtained with a with k_1 of 0.67 ml min^{-1} mg of cells^{-1}. Inset, effect of the k_La on the estimation of the k_1 (◆). (B) Dichloromethane (●) depletion curve obtained with cells expressing sMMO. Transformation followed Michaelis-Menten kinetics, and the data were fitted with equations 6 and 8. Input parameters: H_c = 0.11; k_La, 4.2 min^{-1}; V_g = 94.8 ml; V_l = 25.5 ml; X = 0.19 mg of cells ml^{-1}. An optimal fit was obtained with a K_m of 12 μM and an r_{max} of 0.093 μmol mg of cells^{-1} min^{-1} (solid line). The broken line indicates the fit obtained by assuming first-order kinetics. Inset, effect of the k_La on the estimation of the r_{max} (◇) and K_m (▲).

TABLE 1. Kinetics of transformation of chlorinated hydrocarbons and epoxides with cell suspensions of *Methylosinus trichosporium* OB3b expressing sMMO or pMMO

Substrate	k_1 (ml mg of cells^{-1} min^{-1})[a]	
	Cells expressing pMMO	Cells expressing sMMO
Dichloromethane	0.7 ± 0.1	8.0 ± 0.2
Chloroform	<0.03	1.3 ± 0.1
1,2-Dichloroethane	<0.03	1.0 ± 0.0
VC	1.9 ± 0.2	7.6 ± 0.4
cis-1,2-DCE	0.06 ± 0.02	4.9 ± 0.1
trans-1,2-DCE	0.90 ± 0.0	3.3 ± 0.1
1,1-DCE	<0.03	3.2 ± 0.4
TCE	<0.03	3.1 ± 0.4
cis-1,2-DCE epoxide	ND[b]	0.45 ± 0.05
trans-1,2-DCE	ND	<0.03
Epoxyethane	ND	0.80 ± 0.0
Epoxypropane	ND	<0.03
cis-2,3-Epoxybutane	ND	<0.03
trans-2,3-Epoxybutane	ND	<0.03

[a] Specific first-order rate constants (k_1) were determined in the presence of 20 mM formate. Values given are averages of duplicate measurements.
[b] ND, not determined.

lis-Menten kinetics, the K_m and r_{max} for cells expressing sMMO were determined to be 12 μM and 0.093 μmol min^{-1} mg of cells^{-1}, respectively.

The k_La value for dichloromethane in these experiments was 4.2 min^{-1}. The insets in Fig. 3 show the kinetic parameters that were derived by assuming different k_La values. The results indicated that the terms describing mass transfer in equations 6, 7, and 8 were not significantly influencing the outcome of these experiments. Consequently, it can be concluded that concentrations in the headspace and liquid phase were close to equilibrium.

The values of the specific first-order rate constants that were obtained for various chlorinated compounds are summarized in Table 1. Cells expressing pMMO only showed significant activity with dichloromethane, VC, and *trans*-1,2-DCE. The highest rate was found with VC. The other chlorinated alkanes and alkenes were poorly transformed or not transformed by these cells.

All halogenated alkanes and alkenes tested were transformed by cells expressing sMMO (Table 1). The specific first-order rate constants decreased in the order of dichloromethane, VC, *cis*-1,2-DCE, *trans*-1,2-DCE, 1,1-DCE, TCE, chloroform, and 1,2-dichloroethane.

Formation and degradation of epoxides. Formation of intermediates was observed during transformation of chlorinated ethenes by *Methylosinus trichosporium* OB3b. The intermediates were identified by comparison of retention times, analysis of the products of the reaction with PNBP, and GC-mass spectrometry. The kinetics of formation and degradation were studied.

During transformation of VC, the concomitant generation of an unstable intermediate with a retention time longer than that of VC was observed (Fig. 4A). Mass spectrometry showed the presence of a compound with *m/z* (relative intensity) 78 (53)(M^+), 50 (100)(M^+-28, $CClH_3$), and 43 (53)(M^+-35, C_2H_3O). Mass spectra for VC epoxide have, to our knowledge, not been reported. The spectrum is similar to the spectrum published for chloroacetaldehyde (33), but this compound clearly had a different retention time. These data indicate that the intermediate is VC epoxide. The fragment with *m/z* 50 may have been generated after rearrangement that is likely to occur during mass spectrometric analysis. To confirm that the accumulating intermediate was the epoxide and not one of its degradation products, the compound was trapped with PNBP as described in Materials and Methods. The adduct showed an

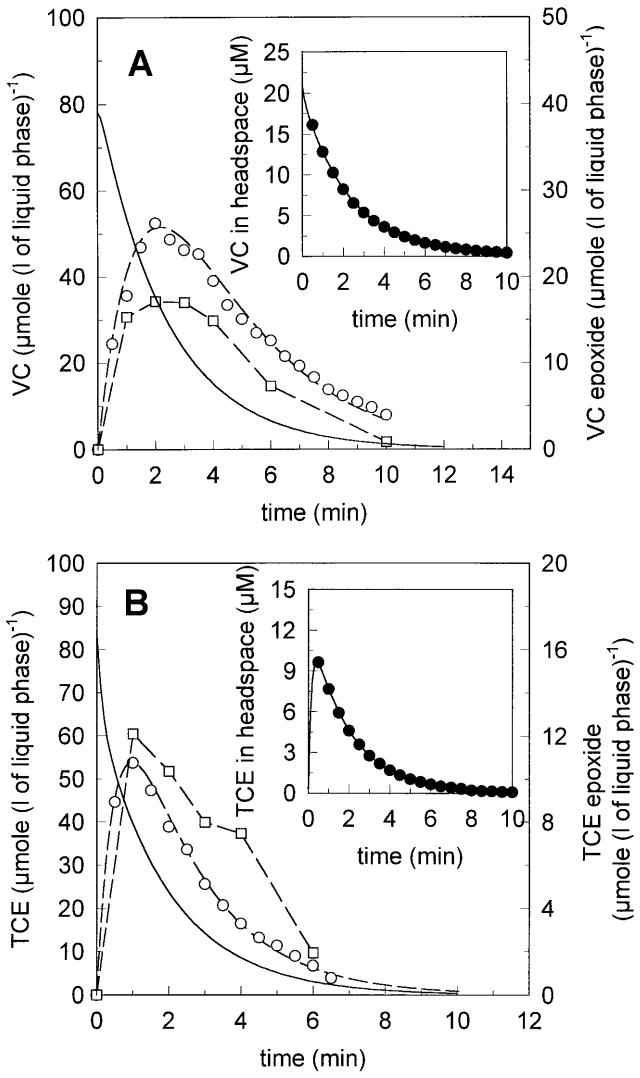

FIG. 4. Generation and degradation of unstable epoxides during degradation of VC and TCE by cell suspensions of *Methylosinus trichosporium* OB3b expressing sMMO. To allow a better comparison between the amount of chlorinated ethene and chlorinated ethene epoxide in the incubation vessel, concentrations are plotted as if all of the substrate was present in the liquid phase. Mass-transfer limitation did significantly influence the course of liquid and headspace concentrations of the chlorinated ethene but not of the corresponding epoxides. The amount of VC epoxide and TCE epoxide per liter of liquid phase was calculated from headspace measurements assuming equilibrium. Insets, headspace concentrations of chlorinated ethene and the fitted substrate depletion curve. (A) GC data of generation and degradation of VC epoxide during degradation of VC. Symbols: ● and solid line, VC; ○, VC epoxide; □, VC epoxide as determined colorimetrically with PNBP. The data obtained by on-line GC analysis were fitted by using equations 6, 7, and 9. Input parameters: $f = 1$; $H_s = 1.26$; $H_o = 0.03$; $V_g = 94.8$ ml; $V_l = 25.5$ ml; $X = 0.49$ mg of cells ml^{-1}. Optimal fits were obtained with a k_1 of 8.1 min^{-1} for VC transformation and a k of 0.53 min^{-1} for VC epoxide degradation. (B) GC data of generation and degradation of TCE epoxide during degradation of TCE. Symbols: ● and solid line, TCE; ○, TCE epoxide; □, TCE epoxide as determined colorimetrically with PNBP. GC data were fitted with equations 6, 7, and 9. Input parameters: $f = 0.94$; $H_s = 0.51$; $H_o = 0.03$; $V_g = 94.8$ ml; $V_l = 25.5$ ml; $X = 0.51$ mg of cells ml^{-1}. Optimal fits were obtained with a k_1 of 3.5 min^{-1} for TCE transformation and a k of 2.0 min^{-1} for TCE epoxide degradation.

absorption maximum (λ_{max}) at 570 nm, which is in close agreement with the value of 560 nm for the PNBP-VC adduct reported by Fox et al. (12).

The Henry coefficient for VC epoxide could not be determined easily and calibration of the GC is difficult, since the compound is unstable in water. However, the epoxide concentrations could be derived by fitting the experimental data (Fig. 4A) with equations 6, 7, and 9 with the following assumptions: (i) conversion of VC results in 100% generation of the corresponding epoxide (12); (ii) the value of the Henry coefficient is between 0.01 and 0.05 (based on the value for related epoxides); and (iii) degradation is a chemical process. From this, it was calculated that the half-life of VC epoxide was approximately 78 s (k = 0.53 min^{-1}). A Henry coefficient of VC epoxide of 0.03 was used in the fits shown in Fig. 4A. A higher Henry coefficient means that a greater fraction of the epoxide is present in the headspace and thus is less susceptible to hydrolysis by water. Changing the value of the Henry coefficient to between 0.01 and 0.05 resulted in less than 3% deviation of the half-life giving the optimal fit, indicating that within this range the obtained half-life is not significantly influenced by the presence of the headspace, since essentially all epoxide is present in the liquid phase. Neglecting of mass-transfer limitation would have influenced the outcome of this experiment since the k_1 of VC transformation would have been significantly underestimated. The low Henry coefficient in combination with a k_La value of 4.3 min^{-1} ensured that epoxide concentrations were close to equilibrium.

The concentration of epoxide derived from these fits will be valid only when the half-life of epoxide is not influenced by the presence of cells due to either aspecific reactions with biomolecules or enzymatic activity, and the diffusion over the membrane is not rate limiting. Concentrations in the liquid phase were determined with PNBP by quenching incubations at different time points with benzene (Fig. 4A). The concentrations obtained with this method were about 40% lower than the concentrations derived from the GC data.

An unstable intermediate was also detected in the headspace during the conversion of TCE (Fig. 4B). Mass spectrometry of this compound yielded fragments with *m/z* (relative intensity) 111 (4)(M^+-35, C_2HCl_2O), 82 (100)(M^+-64, CCl_2), 63 (16)(M^+-83, CClO), 48 (32)(M^+-98, CHCl), and 35 (12)(M^+-111, Cl), which is in agreement with published spectra of TCE epoxide (21). The λ_{max} of the complex with PNBP was 560 nm. Previously, Fox et al. (12) reported a λ_{max} of 520 nm for the complex of PNBP and TCE epoxide. The data were fitted by use of equations 6, 7, and 9, as with VC and VC epoxide, with the exception that oxidation of TCE results in 94% formation of epoxide (12) (Fig. 4B), and thus the half-life of the epoxide was estimated to be 21 s (k = 2.0 min^{-1}). The determination of liquid-phase concentrations with PNBP yielded similar values as the ones derived from headspace analysis, but more scattering occurred, which may be due to the high chemical instability. Neglecting mass-transfer limitation would also have influenced the outcome of this experiment. The k_1 of VC transformation would have been slightly underestimated. Despite the high k value of TCE epoxide degradation, epoxide concentrations in the headspace and liquid phase were close to equilibrium because of the low Henry coefficient combined with a k_La of 3.5 min^{-1}.

Conversion of *trans*-1,2-DCE resulted in a stoichiometric formation of *trans*-1,2-DCE epoxide (data not shown). Mass spectrometry showed the presence of a compound with *m/z* (relative intensity) 112 (13)(M^+), 83 (7)(M^+-29, $CHCl_2$), 63 (3)(M^+-49, CClO), 48 (100)(M^+-64, CHCl), and 35 (6)(M^+, Cl). The values are in agreement with published spectra of chemically synthesized *trans*-1,2-DCE epoxide (14, 18). When 99% of the *trans*-1,2-DCE was degraded, the concentration of *trans*-1,2-DCE epoxide did not decrease significantly for at least 15 min, which was expected since Janssen et al. (18) determined that the half-life of this compound is 31 h.

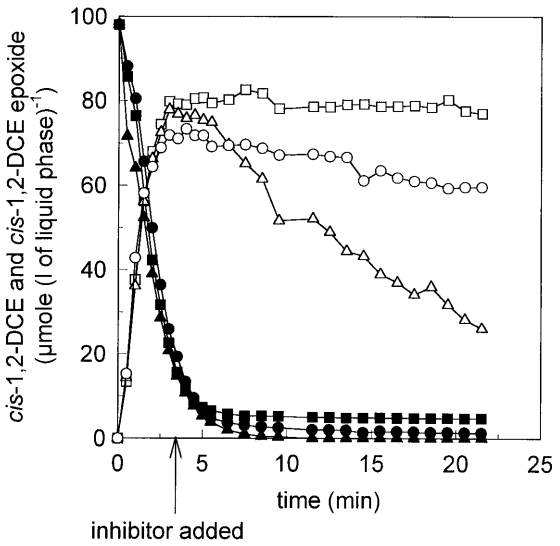

FIG. 5. Formation and degradation of *cis*-1,2-DCE epoxide (open symbols) during transformation of *cis*-1,2-DCE (closed symbols) by resting cell suspensions of *Methylosinus trichosporium* OB3b (0.29 mg of cells ml^{-1}). Symbols: triangles, control; circles, inhibition by 20% CH_4; squares, inhibition by 1% acetylene. Concentrations were calculated assuming equilibrium and plotted as if the substrates were completely dissolved in the liquid phase to allow a better comparison between the amounts of *cis*-1,2-DCE and *cis*-1,2-DCE epoxide.

During conversion of 1,1-DCE, no intermediate accumulated in the headspace. The epoxide that is presumably generated by oxidation by sMMO is very unstable and to our knowledge has never been detected in biological systems.

Conversion of *cis*-1,2-DCE resulted in the concomitant generation of *cis*-1,2-DCE epoxide (Fig. 5). Mass spectrometry showed the presence of a compound with *m/z* (relative intensity) 112 (10)(M^+), 83 (7)(M^+-29, $CHCl_2$), 63 (3)(M^+-49, CClO), 48 (100)(M^+-64, CHCl), and 35 (7)(M^+, Cl). The values are in agreement with published spectra of chemically synthesized *cis*-1,2-DCE epoxide (14, 18).

After degradation of approximately 80% of the *cis*-1,2-DCE, the concentration of *cis*-1,2-DCE epoxide started to decrease again. This suggested that the epoxide was actively degraded, since it is known to be relatively stable in aqueous solutions, with a half-life of approximately 72 h (18). In a parallel experiment $HgCl_2$, a potent inhibitor of biological activity was added 3.5 min after the conversion of *cis*-1,2-DCE was started. This immediately stopped the conversion of both *cis*-1,2-DCE and *cis*-1,2-DCE epoxide, confirming that the epoxide was degraded biologically. Inhibition of sMMO activity with acetylene, a specific inhibitor of MMO (30, 34), also completely stopped the degradation of these compounds (Fig. 5). This indicated that *cis*-1,2-DCE epoxide was converted by sMMO. Biologically synthesized *cis*-1,2-DCE epoxide was added to a cell suspension freshly harvested from the fermentor to determine the transformation kinetics. The specific first-order rate constant of this conversion was 0.45 ml min^{-1} mg of $cells^{-1}$.

We tested whether other epoxides were also a substrate for cells expressing sMMO. The transformation rate of *trans*-1,2-DCE epoxide was below the detection limit of 0.03 ml min^{-1} mg of $cells^{-1}$. Of the nonchlorinated epoxides that were tested,

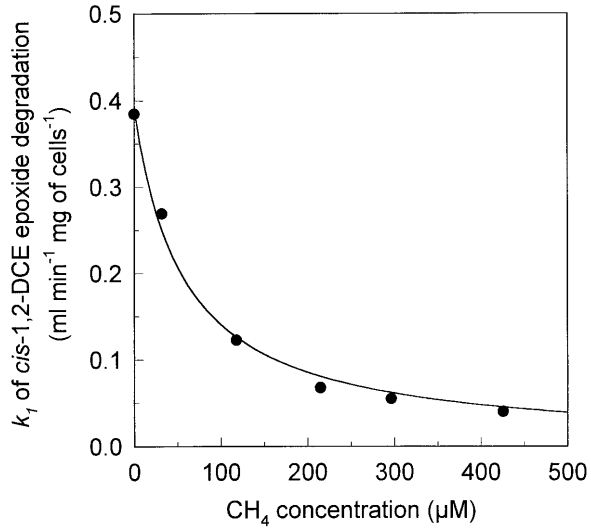

FIG. 6. Inhibition of the transformation of *cis*-1,2-DCE epoxide by methane. Cell suspensions contained 0.42 mg of cells of *Methylosinus trichosporium* OB3b expressing sMMO ml^{-1}. Specific first-order transformation rate constants in the presence of various liquid-phase concentrations of methane were calculated. The data were fitted with equation 11, yielding values of $k_{1.0}$ of 0.39 ml min^{-1} mg of cells^{-1} and K_i of 56 μM.

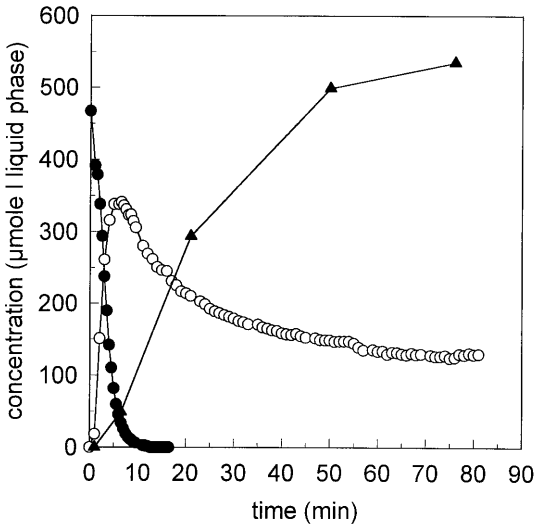

FIG. 7. Transformation of *cis*-1,2-DCE (●), generation and degradation of *cis*-1,2-DCE epoxide (○), and liberation of chloride (▲) by cell suspensions of *Methylosinus trichosporium* OB3b (0.8 mg of cells ml^{-1}). Concentrations were calculated assuming equilibrium and plotted as if the substrates were completely dissolved in the liquid phase to allow comparison between the amounts of *cis*-1,2-DCE, *cis*-1,2-DCE epoxide, and chloride.

only epoxyethane was transformed with a k_1 of 0.8 ml min^{-1} mg of cells^{-1}. For the structurally related epoxides epoxypropane, *cis*-2,3-epoxybutane, and *trans*-2,3-epoxybutane, the k_1 values were below the detection limit of 0.03 ml min^{-1} mg of cells^{-1}.

Addition of the natural substrate of sMMO, methane, lowered the degradation rate of *cis*-1,2-DCE epoxide, indicating competition for the same enzyme by the two compounds. The kinetics of inhibition of the conversion of *cis*-1,2-DCE epoxide by methane was studied by determining the k_1 values at various methane concentrations (Fig. 6). The data were fitted with equation 11, and an optimal fit was obtained by with a K_i of 56 μM. Values of K_s and K_m for methane degradation found are 40 μM (6a) and 92 μM (27), respectively.

Conversion of *cis*-1,2-DCE epoxide appeared to inactivate the cells, resulting in decreasing degradation rates. This indicates that the oxidation product of *cis*-1,2-DCE epoxide is a highly reactive compound (Fig. 7). A limitation in formate or O_2 is not the cause of this decrease, since cells did not lose activity in control incubations after 2 h (data not shown). Chloride levels were determined during the degradation of *cis*-1,2-DCE and *cis*-1,2-DCE epoxide (Fig. 7), since this is one of the possible products of the conversion of *cis*-1,2-DCE epoxide. Chloride was indeed liberated during the conversion of *cis*-1,2-DCE epoxide. At the end of the experiment, 57% of the chlorine added as *cis*-1,2-DCE was present as inorganic chloride. At this time, degradation rates of *cis*-1,2-DCE epoxide had almost stopped, and 28% of the chlorine was present as *cis*-1,2-DCE epoxide. The remaining 15% might be present in nonvolatile chlorinated compounds or in adducts to cellular components.

DISCUSSION

Sorption, laborious extraction procedures, and high volatility may interfere with the reliable estimation of microbial transformation rate constants for halogenated aliphatic compounds. The on-line monitoring of headspace concentrations with GC described in this paper enabled the rapid determination of conversion rates at practically relevant low substrate concentrations and allowed identification of unstable intermediates. Mass-transfer limitation and sorption may influence the measurements and therefore these factors were carefully analyzed to ensure that kinetic parameters were determined accurately.

The transformation rates with cells expressing pMMO or sMMO were determined. The k_1 values found for 1,2-dichloroethane, TCE, *cis*-1,2-DCE, and *trans*-1,2-DCE of cells expressing sMMO are similar to those reported by Oldenhuis et al. (27). The value of k_1 for 1,1-DCE reported previously was threefold lower than the value of 3.2 ml min^{-1} mg of cells^{-1} that we found, which may be due to rapid inactivation of the cells (38a). The value of k_1 for chloroform of 1.3 ml min^{-1} mg of cells^{-1} is much lower than the value of 16 min^{-1} mg of cells^{-1} determined previously (28). Few data are available about the transformation kinetics of chlorinated compounds by cells expressing pMMO. Complete degradation of 0.2 mM 1,2-dichloroethane and chloroform was observed previously during 24 h of incubation with cell suspensions of *Methylosinus trichosporium* OB3b expressing pMMO (0.3 to 0.4 mg of cells ml^{-1}) (28). However, in this study, we found that the transformation rates of these compounds were below the detection limit of 0.03 ml min^{-1} mg of cells^{-1}.

Strain OB3b, grown either in the presence or absence of copper, is capable of transformation of VC. Under anaerobic conditions, the degradation rate of chlorinated ethenes decreases with increasing number of chlorine substituents (8, 39). Hence, *cis*-1,2-DCE and VC often accumulate during anaerobic degradation of perchloroethene under field conditions, and these compounds are frequently detected in groundwater that was originally contaminated with perchloroethene. *Mycobacterium* sp. strain L1 is the only strain described to date which utilizes VC as a sole source of carbon and energy (16), but the instability of enzymes involved in VC metabolism in this strain does not favor its application in a bioremediation process. Removal of VC with activated carbon is also less efficient compared with removal of higher chlorinated ethenes, making

aerobic methods using methanotrophs for the treatment of waste streams contaminated with VC an attractive option.

The transformation rates obtained with *Methylosinus trichosporium* OB3b are among the highest observed for cometabolism. Dichloromethane, 1,2-dichloroethane, and VC can also serve as sole sources of carbon and energy for specialized strains. The k_1 for organisms growing on these compounds can be derived from the specific growth rate, the Monod constant, and the yield by using $k_1 = \mu_{max}/YK_s$. This allows the comparison of the degradation rates of these organisms with the cometabolic degradation rates determined for *Methylosinus trichosporium* OB3b. The values for k_1 for 1,2-dichloroethane that can thus be calculated for *Xanthobacter autotrophicus* GJ10 and *Ancylobacter aquaticus* AD25, 0.3 and 3.0 ml min^{-1} mg of $cells^{-1}$, respectively (38), are similar to the value that we found for *Methylosinus trichosporium* OB3b. *Mycobacterium* sp. strain L1 degraded VC with an approximately twofold-higher k_1 (16) as that found by us for cometabolic transformation with *Methylosinus trichosporium* OB3b. The higher k_1 value, 53 ml min^{-1} mg of $cells^{-1}$, that can be calculated for dichloromethane degradation by *Hyphomicrobium* sp. strain GJ21 (7) in comparison with the cometabolic degradation rate of *Methylosinus trichosporium* OB3b expressing sMMO or pMMO is due mainly to the low-affinity constant, 10 μM, of strain GJ21.

The on-line analysis of headspace concentrations also made it possible to study the formation and degradation of the corresponding epoxides. The accumulation of epoxides was observed during transformation of all chlorinated ethenes except 1,1-DCE. The somewhat different λ_{max} values that we found for the PNBP adducts of the epoxides in this study compared with the values reported by Fox et al. (12) may be due to the use of benzene in the previous study for extraction of the epoxides whereas we directly trapped the epoxide in ethylene glycol in which PNBP was dissolved. The half-lives that we determined for VC epoxide, 78 s, and TCE epoxide, 21 s, are in good agreement with the values of 1.5 min (20) and 12 s (25), respectively, found in the absence of cells, indicating that these compounds are mainly chemically degraded. Our results show that during transformation of pulses of VC and TCE, the corresponding epoxides accumulate in the medium at significant concentrations before they disappear as a result of spontaneous hydrolysis, rearrangement reactions, or reactions with biomolecules.

To our knowledge, this is the first time that TCE epoxide has been detected in a microbial whole-cell system. Previously, TCE epoxide formation has only been reported as occurring during oxidation of TCE in vitro by purified sMMO by Fox et al. (12), who found that 94% of the TCE that was oxidized was converted to TCE epoxide. Both TCE epoxide and some of its degradation products, such as acyl chlorides, are highly reactive compounds that rapidly react with nucleophiles (21). The covalent modification of cellular components by these compounds limits the transformation capacity of cell suspensions (1, 27). Experiments using ^{14}C-labelled TCE revealed that TCE conversion products reacted nonspecifically with cellular components but not with methanol dehydrogenase, which suggested that the epoxide may not reach the periplasm (27). The results found here indicate that the epoxide must leave the cell and diffuse through the periplasm. Recently, it was reported that glucose fermentation by yeast cells was inhibited in the presence of *Xanthobacter* Py2 cells degrading TCE, indicating that toxic metabolites occurred in the medium (32).

cis-1,2-DCE is an important groundwater pollutant that is generated from perchloroethene and TCE by dechlorination under anaerobic conditions. However, few data about the aerobic degradation of *cis*-1,2-DCE are available compared with the data about degradation of other chlorinated ethenes. We found that *cis*-1,2-DCE epoxide formed by oxidation of *cis*-1,2-DCE is actively degraded by cells expressing sMMO. The effect of methane and acetylene and the competitive inhibition of *cis*-1,2-DCE epoxide degradation by methane strongly indicated that sMMO was involved. Surprisingly, epoxyethane was also degraded, while related epoxides such as epoxypropane *cis*-2,3-epoxybutane, *trans*-2,3-epoxybutane, and *trans*-1,2-DCE epoxide were not substrates for these cells, suggesting that unlike for halogenated alkenes and alkanes, the substrate range of sMMO for epoxides is rather small. The nature of the reaction is not clear. Lewis acid-like interactions catalyzed by the heme iron in its Fe(III) state have been postulated to cause the rearrangement of TCE epoxide to chloral in cytochrome P-450 (17). It is unlikely that a similar mechanism holds for the conversion of *cis*-1,2-DCE epoxide by the diferrous cluster in sMMO, since a rearrangement of the epoxide to dichloroacetaldehyde is inconsistent with the liberation of chloride that was observed.

Castro et al. (6), using ^{13}C and ^{14}C nuclear magnetic resonance suggested that the VC epoxide that is formed after the oxidation of VC by *Methylosinus trichosporium* OB3b is further degraded via three different pathways. The major pathway was reduction to epoxyethane and a subsequent hydrolysis to ethylene glycol. They postulated that both reactions are catalyzed by the organism. However, the epoxides were not detected, probably because the steady-state concentrations were too low. VC epoxide might also be hydrolyzed biologically or chemically, yielding glycolaldehyde, or chemically rearranged to chloroacetaldehyde.

The toxicity of chlorinated ethene epoxides and their degradation products suggests that active conversion to nonreactive compounds may reduce or prevent such toxic effects. However, no activity of microbial enzymes that are involved in the metabolism of epoxides with chlorinated ethene epoxides has been reported. The conversion of *cis*-1,2-DCE epoxide catalyzed by sMMO does not seem to reduce toxic effects, since the conversion clearly inactivated the cells.

ACKNOWLEDGMENTS

The work of Johan E. T. van Hylckama Vlieg was financed by grant IOP91204 from the Dutch IOP Environmental Biotechnology Program, and the work of Wim de Koning was financed by grant EVSV-CT92-0239 from the European Community.

Piet Wietzes and Jos van der Ven are acknowledged for technical support and assistance in nuclear magnetic resonance analysis, respectively.

REFERENCES

1. **Alvarez-Cohen, L., and P. McCarthy.** 1991. Effects of toxicity aeration and reductant supply on trichloroethylene transformation by a mixed methanotrophic culture. Appl. Environ. Microbiol. **57:**228–235.
2. **Arciero, D., T. Vanelli, T. M. Logan, and A. B. Hooper.** 1989. Degradation of trichloroethylene by the ammonia oxidizing bacterium *Nitrosomonas europaea*. Biochem. Biophys. Res. Commun. **159:**640–643.
3. **Arvin, E.** 1991. Biodegradation kinetics of chlorinated aliphatic hydrocarbons with methane oxidizing bacteria in an aerobic fixed biofilm reactor. Water Res. **25:**873–881.
4. **Barbin, A., H. Brésil, A. Croisy, P. Jacquignon, C. Malaveille, R. Montesano, and H. Bartsch.** 1975. Liver-microsome-mediated formation of alkylating agents from vinyl bromide and vinyl chloride. Biochem. Biophys. Res. Commun. **67:**596–603.
5. **Bergmann, J. G., and J. Sanik.** 1957. Determination of trace amounts of chloride in naphtha. Anal. Chem. **29:**241–243.
6. **Castro, C. E., D. M. Riebeth, and N. O. Belser.** 1992. Biodehalogenation: the metabolism of vinyl chloride by *Methylosinus trichosporium* OB-3b. A sequential oxidative and reductive pathway through chloroethylene oxide. Environ. Toxicol. Chem. **11:**749–755.

6a. **de Koning, W.** Unpublished data.

7. **Diks, R. M. M.** 1992. Ph. D. thesis. Technical University of Eindhoven, Eindhoven, The Netherlands.

8. **DiStefano, T. D., J. M. Gossett, and S. H. Zinder.** 1991. Reductive dechlorination of high concentrations of tetrachloroethene to ethene by an anaerobic-enrichment culture in the absence of methanogenesis. Appl. Environ. Microbiol. **57:**2287–2292.
9. **Ensign, S. A., M. R. Hyman, and D. A. Arp.** 1992. Cometabolic degradation of chlorinated alkanes by alkene monooxygenase in a propylene-grown *Xanthobacter* strain. Appl. Environ. Microbiol. **58:**3038–3046.
10. **Ewers, J., W. Clemens, and H. J. Knackmuss.** 1990. Selection of trichloroethylene (TCE) degrading bacteria that resist inactivation by TCE. Arch. Microbiol. **154:**410–413.
11. **Fennell, D. E., Y. M. Nelson, S. E. Underhill, T. E. White, and W. J. Jewell.** 1993. TCE degradation in a methanotrophic attached-film bioreactor. Biotechnol. Bioeng. **26:**859–872.
12. **Fox, B. G., J. G. Borneman, L. P. Wackett, and J. D. Lipscomb.** 1990. Haloalkene oxidation by the soluble methane monooxygenase from *Methylosinus trichosporium* OB3b: mechanistic and environmental implications. Biochemistry **29:**6419–6427.
13. **Gossett, J. M.** 1987. Measurement of Henry's law constants for C_1 and C_2 chlorinated hydrocarbons. Environ. Sci. Technol. **21:**202–208.
14. **Griesbaum, K., R. Kibar, and B. Pfeffer.** 1975. Synthese und stabilität von 2,3-dichloroxiranen. Liebigs Ann. Chem. **75:**214–224.
15. **Guengerich, F. P., W. M. Crawford, and P. G. Wanatabe.** 1979. Activation of vinylchloride to covalently bound metabolites: roles of 2-chloroethylene oxide and 2-chloroacetaldehyde. Biochemistry **18:**5177–5182.
16. **Hartmans, S., and J. A. M. de Bont.** 1992. Aerobic vinyl chloride metabolism in *Mycobacterium* L1. Appl. Environ. Microbiol. **58:**1220–1226.
17. **Henschler, D., W. R. Hoos, H. Fetz, E. Dallmeier, and M. Metzler.** 1979. Reactions of trichloroethylene epoxide in aqueous systems. Biochem. Pharmacol. **28:**543–548.
18. **Janssen, D. B., G. Grobben, R. Hoekstra, R. Oldenhuis, and B. Witholt.** 1988. Degradation of *trans*-1,2-dichloroethene by mixed cultures of methanotrophic bacteria. Appl. Environ. Biotechnol. **29:**392–399.
19. **Janssen, D. B., A. Scheper, L. Dijkhuizen, and B. Witholt.** 1985. Degradation of halogenated aliphatic compounds by *Xanthobacter autotrophicus* GJ10. Appl. Environ. Microbiol. **49:**673–677.
20. **Kline, S. A., J. J. Solomon, and B. L. Van Duuren.** 1978. Synthesis and reactions of chloroalkene epoxides. J. Org. Chem. **43:**3596–3600.
21. **Kline, S. A., and B. L. Van Duuren.** 1977. Reactions of epoxy-1,1,2-trichloroethane with nucleophiles. J. Heterocycl. Chem. **14:**455–458.
22. **Kohler-Staub, D., and T. Leisinger.** 1985. Dichloromethane dehalogenase of *Hyphomicrobium* sp. strain DM2. J. Bacteriol. **162:**676–681.
23. **Landa, A. S., M. E. Sipkema, J. Weijma, A. A. C. M. Beenackers, J. Dolfing, and D. B. Janssen.** 1994. Cometabolic degradation of trichloroethylene by *Pseudomonas cepacia* G4 in a chemostat with toluene as the primary substrate. Appl. Environ. Microbiol. **60:**3368–3374.
24. **Maltoni, C., and G. Lefemine.** 1974. Carcinogenicity bioassays of vinyl chloride. I. Research plan and early results. Environ Res. **7:**387–405.
25. **Miller, R. E., and F. P. Guengerich.** 1982. Oxidation of trichloroethylene by liver microsomal cytochrome P-450: evidence for chlorine migration in a transition state not involving trichloroethylene epoxide. Biochemistry **21:** 1090–1097.
26. **Nelson, M. J. K., S. O. Montgomery, W. R. Mahaffey, and P. H. Pritchard.** 1987. Biodegradation of trichloroethylene and involvement of an aromatic pathway. Appl. Environ. Microbiol. **53:**949–954.
27. **Oldenhuis, R., J. Y. Oedzes, J. J. van der Waarde, and D. B. Janssen.** 1991. Kinetics of chlorinated hydrocarbon degradation by *Methylosinus trichosporium* OB3b and toxicity of trichloroethylene. Appl. Environ. Microbiol. **57:** 7–14.
28. **Oldenhuis, R., R. L. J. M. Vink, D. B. Janssen, and B. Witholt.** 1989. Degradation of chlorinated aliphatic hydrocarbons by *Methylosinus trichosporium* OB3b expressing soluble methane monooxygenase. Appl. Environ. Microbiol. **55:**2819–2826.
29. **Perry, R. H., D. W. Green, and J. O. Maloney.** 1984. Perry's chemical engineers handbook, 6th ed., table 3-137. McGraw-Hill Book Co., Singapore.
30. **Prior, S. D., and H. Dalton.** 1985. Acetylene as a suicide substrate and active site probe for methane monooxygenase from *Methylococcus capsulatus* (Bath). FEMS Microbiol. Lett. **29:**105–109.
31. **Rannug, U., A. Johansson, C. Ramel, and C. A. Wachtmeister.** 1974. The mutagenicity of vinyl chloride after metabolic activation. Ambio **6:**194–197.
32. **Reij, M. W., J. Kieboom, J. A. M. de Bont, and S. Hartmans.** 1995. Continuous degradation of trichloroethylene by *Xanthobacter* sp. strain Py2 during growth on propene. Appl. Environ. Microbiol. **61:**2936–2942.
33. **Stenhagen, E., S. Abrahamnon, and F. W. McLafferty.** 1969. Atlas of mass spectral data. Interscience Publishers, New York.
34. **Stirling, D. I., and H. Dalton.** 1979. Properties of the methane monooxygenases from extracts of *Methylosinus trichosporium* OB3b and evidence for its similarity to the enzyme from *Methylococcus capsulatus* (Bath). Eur. J. Biochem. **96:**205–212.
35. **Sung-Cheol, K., J. P. Bowman, and G. S. Sayler.** 1993. Soluble methane monooxygenase production and trichloroethylene degradation by a type I methanotroph, *Methylomonas methanica* 68-1. Appl. Environ. Microbiol. **59:**960–967.
36. **Tschantz, M. F., J. P. Bowman, T. L. Donaldson, P. R. Bienkowski, J. M. Strong-Gunderson, A. V. Palumbo, S. E. Herbes, and G. S. Sayler.** 1995. Methanotrophic TCE biodegradation in a multi-stage bioreactor. Environ. Sci. Technol. **29:**2073–2082.
37. **Tsien, H. C., G. A. Brusseau, R. S. Hansson, and L. P. Wackett.** 1989. Biodegradation of trichloroethylene by *Methylosinus trichosporium* OB3b. Appl. Environ. Microbiol. **55:**3155–3161.
38. **Van den Wijngaard, A. J., R. D. Wind, and D. B. Janssen.** 1993. Kinetics of bacterial growth on chlorinated aliphatic compounds. Appl. Environ. Microbiol. **59:**2041–2048.

38a. **van Hylckama Vlieg, J. E. T.** Unpublished data.

39. **Vogel, T. M., and P. L. McCarthy.** 1985. Biotransformation of tetrachloroethylene to trichloroethylene, dichloroethylene vinyl chloride, and carbon dioxide under methanogenic conditions. Appl. Environ. Microbiol. **49:**1080–1083.
40. **Wackett, L. P., G. A. Brusseau, S. R. Householder, and R. S. Hanson.** 1989. Survey of microbial oxygenases: trichloroethylene degradation by propane-oxidizing bacteria. Appl. Environ. Microbiol. **55:**2960–2964.
41. **Wackett, L. P., and D. T. Gibson.** 1988. Degradation of trichloroethylene by toluene dioxygenase in whole-cell studies with *Pseudomonas putida* F1. Appl. Environ. Microbiol. **54:**1703–1708.